Iraqi Journal of Physics, 2024 *Vol. 22, No. 3, PP. 27-36*
https://doi.org/10.30723/ijp.v22i3.1241 *P-ISSN: 2070-4003*
E-ISSN: 2664-5548

Study of Some Physical and Antibacterial Properties of Bio-based (PLA)/(PCL) Blend Reinforced with ZrO_2 Nanoparticles

Hassan A. Ashoor[1a*] and Awattif A. Mohammed[1b]
[1]*Department of Physics, College of Science, University of Baghdad, Baghdad, Iraq*
[b]E-mail: awattif.mohammed@sc.uobaghdad.edu.iq
[a*]Corresponding author: hasan.ali1604a@sc.uobaghdad.edu.iq

Abstract

The aim of this study was to produce flexible films by combining polylactic acid (PLA) and poly(ε-caprolactone) (PCL), and enhance their strength by reinforcing them with different weight percentages (0.75, 1.5, and 2.25%) of zirconium oxide (ZrO_2) nanoparticles (NPs) using a solvent casting process. The physical and antibacterial properties of the films were analysed to determine their suitability for use in food packaging. X-ray diffraction (XRD) patterns of the PLA/PCL films containing 2.25% by weight ZrO_2 nanoparticles have a peak at an angle of $2\theta = 17.18°$, accompanied by smaller peaks. This confirms that these thin films have a semi-crystalline structure and that the molecules in the thin films are well dispersed. Scanning electron microscopy (SEM) analysis of the film surfaces reveals that the pure PLA/PCL films exhibit a smooth surface, while the PLA/PCL/ZrO_2NPs films have a rough surface. The thermal behaviour of the blends through differential scanning calorimetry (DSC) showed fluctuations due to variations in the reinforcement ratio, resulting in changes in the glass transition and melting temperatures. These oscillations indicate changes in the level of crystallinity. ZnO_2 has antibacterial properties that promote growth inhibition, making these films more effective in food packaging.

Article Info.

Keywords:
Polylactic Acid, Polycaprolactone, Antibacterial, Food Packaging, Bioblend.

Article history:
Received: Feb. 02, 2024
Revised: May, 02, 2024
Accepted: May,26, 2024
Published: Sep. 01, 2024

1. Introduction

Fossil-based polymers are often used in many applications because of their remarkable physicochemical properties, lightweight composition, affordability, ease of processing and adaptability. They have applications in various sectors, such as healthcare, agriculture, packaging, commodities, electronics, and structural fields like automotive, maritime, aerospace, and civil engineering. However, the overuse of these compounds resulted in substantial ecological problems since they do not readily break down via natural processes [1, 2]. Biodegradable polymers undergo complete disintegration of their physical and chemical properties when exposed to environmental elements, such as soil and microorganisms, water, or sunshine. These compounds may be categorized as either natural or manufactured, and they completely break down into water (H_2O), carbon dioxide (CO_2), and biomass when they are disposed of in the environment [3, 4]. The increase in the use of packaging and other temporary uses and the resulting impact on the environment have become a subject of public concern [5]. The widespread use of biodegradable polymers in many applications may be attributed to the biotechnologies progress, increased public awareness, improved manufacturing methods, and lower global production costs. As a consequence of the need to find polymers that are not sourced from fossil fuels, there has been a significant increase in worldwide interest in biodegradable polymers [6, 7]. Conventional polymers are on the verge of being substituted, although they currently represent a minor proportion of the world plastics industry [8].

Polylactic acid (PLA) is a highly regarded biodegradable polymer that has been extensively studied and is now being produced on a large scale in industry [9]. Over the last twenty years, PLA has been extensively used in several typical applications, especially in food packaging. However, the material's fragility and lack of robustness limit its use in other industries that often use flexible polymers [10, 11]. The advantage of polymer engineering is the exact control and modification of its physico-chemical properties. Conventional methods to overcome certain limitations in the field of polymers include blending polymers with other substances, carrying out copolymerization or crosslinking, using inert or beneficial fillers, or utilizing a combination of these techniques [12, 13].

Poly(ε-caprolactone) (PCL) is a pliable and environmentally degradable thermoplastic polyester that shows promise as a suitable blend with PLA. PCL is now being investigated for several uses, spanning from its use in packaging to its potential as drug delivery vehicles or medical implants. PCL may be fabricated into various shapes by extrusion, injection moulding, and stringing techniques. By carefully choosing a filler and/or a compatibilizer, it is possible to tailor the final morphology, miscibility, and properties of polymer blends [14-16]. Therefore, the properties of the optimal biodegradable blends may be tailored to achieve a certain degree of performance. Previous scientific studies have investigated the integration of PCL with PLA to reduce its initial modulus and yield stress [17]. The addition of PCL significantly enhances the toughness of PLA, leading to a substantial increase in the required energy for sample fracture [18].

The kinetics and speed of crystallization can be precisely controlled by varying the ratios of PLA and PCL in the blends [19]. Therefore, PLA/PCL blends may be used as a durable and environmentally beneficial alternative to current polymers produced from petroleum, such as polypropylene, high-density polyethylene, and polystyrene [20].

The desired attributes of PLA and PCL have stimulated investigations into PLA/PCL blends, with the potential inclusion of a nanofiller as a third component to improve the blend's compatibility and overall properties. In recent years, there has been a significant increase in the number of technical, scientific, and medicinal applications for nanoparticles [21, 22].

Adding certain metal oxides, such as Al_2O_3, SiO_2, TiO_2, ZnO, and zirconium oxide (ZrO_2), significantly enhances its properties [23]. ZrO_2 has several desired characteristics, including high hardness, excellent mechanical strength, and good resistance to wear, chemicals, and ions [24].

Castro et al. synthesized four block formulations using zinc oxide nanoparticles (ZnO-NPs), PLA, and PCL to promote subdermal tissue regeneration. The composition of the composites was confirmed by X-ray diffraction (XRD) and Fourier transform infrared spectroscopy (FT-IR). Thermogravimetric (TGA) and differential scanning calorimetry (DSC) analyses confirmed that the ZnO-NPs bind to the carbonyl groups of the polymer, leading to the formation of fragmentation sites in the polymer's backbone. Scanning electron microscopy (SEM) showed that increasing the amount of ZnO-NPs improved the dispersion and homogeneous accumulation of the polymeric chains. This led to a more compact surface, resulting in the observed shape [25].

Swaroop and Shukla used the solvent casting method to produce flexible films based on PLA incorporated with polyethylene glycol (PEG) and reinforced with MgO nanoparticles. They examined the fundamental mechanical, antibacterial, and optical properties of the films for their use in food packaging. The 2 wt% PLA/PEG/MgO films exhibited an elongation at break that was about 760% greater than that of the pure PLA films. Adding PEG and MgO nanoparticles to PLA sheets resulted in a significant

alteration in their optical properties. Furthermore, as compared to ordinary PLA films, PLA/PEG/MgO has shown a substantial enhancement in antibacterial efficacy, thereby confirming PLA/PEG/MgO as a proficient material for packaging films [26].

The current work prepared biofilms made of bioblends PLA, PCL, and ZrO_2NPs for use in packaging and food packaging.

2. Experimental Work

2.1. Materials

PLA was provided by BASF India limited. It has a density of 1.25 g/cm^3. PCL was purchased from Sigma-Aldrich. The Tetrahydrofuran (THF) solution was purchased from HiMedia laboratories Pvt. Ltd., India. SkySpring nanomaterials-USA provided the ZrO_2 nanoparticles.

2.2. Samples Preparation

To obtain a PLA solution, 2.1g of PLA (weighted using an electron balance of four digits) was dissolved in THF with heating at 55°C for 2 hrs and stirring using a magnetic stirrer until the solution became viscous. In the same way, PCL solution was prepared with 0.9g PCL. The two solutions of PLA and PCL were mixed using a magnetic stirrer and then cast into a petri dish of 12cm diameter at room temperature for 24 hr to ensure complete solvent removal. Nanocomposite films were prepared by solution-cast film samples of the biodegradable material (PLA/PCL) reinforced with different concentrations of ZrO_2NPs (0.75, 1.5, and 2.25 wt%). The nanocomposite solutions were dissolved in THF with stirring using a magnetic stirrer and then cast onto petri dishes to generate films after solvent evaporation at room temperature. Then cast on the glass petri dishes and kept at 50°C in the vacuum oven at 24°C to ensure complete solvent removal. The thickness of PLA/PCL/ZrO_2NPs film was 110 µm, determined using an electronic digital micrometre (EDM).

2.3. Characterization

The XRD patterns were obtained using a Philips PW1730 diffractometer from the Netherlands. The instrument was supplied with Cu-Ka radiation (λ = 1.540562 Å) and operated at 40 kV. The Bragg's angle (2θ) was measured in the range of 4–80°. The film morphology was assessed using a Tescan MIRA III SEM from the Czech Republic, operated at an accelerating voltage of 200 kV. To mitigate the impact of the electron beam on the charge of the samples, a vacuum evaporation process was employed to apply a thin layer of gold to the samples' surfaces. The TA Q600 is an American DSC that operates in a nitrogen atmosphere and is specifically designed for the device. During the DSC, the samples underwent heating and scanning. To ensure the absence of any previous thermal effects, the samples were heated at a controlled rate of 23°C per minute, reaching a temperature range of 0 to 1000°C. This process lasted for a total of 10 minutes. The scanning method recorded the melting properties of the material throughout the process of reheating.

The antibacterial activity was examined in this work using the agar diffusion technique. Six plates were contaminated with 0.1 ml of a bacterial solution comprising E. coli and S. aureus (at concentrations of 1 and 5 wt%, respectively) in a 30 ml volume of plate count agar. The diameter of the inhibitory zone was measured in mm after a 24 hr incubation period at 37 ºC.

3. Results and Discussion

3.1. XRD

Blend constructions consisting of PLA, PCL, and ZrO_2NPs strongly depend on the semi-crystalline properties of the polymers for their main mechanical, barrier, and thermal features. Therefore, it is crucial to investigate these issues. Fig. 1 and Table 1 display the XRD patterns of the pure PLA/PCL blend and that with 0.75 and 2.25wt% ZrO_2NPs. Pure PLA/PCL films exhibited a prominent peak at 2θ of about 17.86°, as shown in Table 1, indicating their semi-crystalline structure. On the other hand, the PLA/PCL/0.75wt%ZrO_2NPs film showed a broad peak, indicating their completely amorphous composition, in addition to less clear peaks at 2θ =17.49°, 28.25° and 31.50° indexed as 100, 111, and -111, respectively according to JCPDS card (00-007-0343). The PLA/PCL/2.25wt%ZrO_2NPs film showed a prominent peak in addition to less clear peaks at 2θ =17.18°, 28.15° and 41.88° indexed as 100, -111, and -121, respectively according to JCPDS card (00-013-0307). This indicates that the prepared PLA/PCL/ZrO_2NPs films have a semi-crystalline structure. The structure of ZrO_2NPs was monoclinic [27].

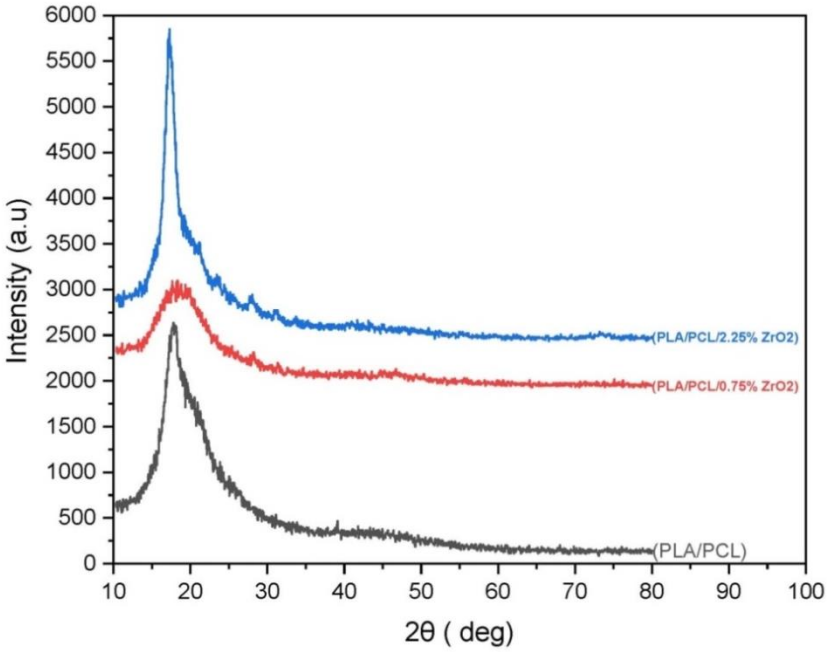

Figure 1: XRD for the pure PLA/PCL blend film and for PLA/PCL/0.75, 2.25 wt%ZrO_2NP).

Table 1: XRD parameters of the pure PLA/PCL, and PLA/PCL/ZrO_2NPs films.

Sample	Pos. [2θ]	Height [cts]	FWHM Left [2θ]	d-spacing	Rel. Int. [%]	Tip Width
Pure PLA/PCL)	17.8600	1780.31	1.6800	4.96239	100.00	2.0160
PLA/PCL/0.75%ZrO_2	17.4970	709.55	3.5424	5.06871	98.53	4.2509
	19.8051	720.13	1.9680	4.48291	100.00	2.3616
	28.2505	126.12	0.5904	3.15903	17.51	0.7085
	31.5004	41.98	0.5904	2.84014	5.83	0.7085
	46.1586	44.12	3.1488	1.96665	6.13	3.7786
PLA/PCL/2.25%ZrO_2	17.1827	2929.83	0.1968	5.16071	100.00	0.2362
	21.2514	677.21	0.5904	4.18097	23.11	0.7085
	28.1591	176.12	1.1808	3.16908	6.01	1.4170
	41.8832	23.07	4.7232	2.15697	0.79	5.6678
	73.6438	40.53	1.1808	1.28633	1.38	1.4170

3.2. SEM

Figs. 2, 3, 4 and 5 show the SEM images of the prepared films. To capture more detailed surface properties, microscopic images of PLA/PCL/ZrO_2NPs and pure PLA/PCL films were obtained at 500 nm and 100 nm resolution, respectively, as shown in the inset. A surface study of the films revealed that the pure PLA/PCL films exhibited a smooth and dense surface, but PLA/PCL/ZrO_2NPs films have an irregular surface due to the presence of the nanoparticles. The prepared films PLA/PCL/0.75, 1.5, and 2.25 wt%ZrO_2 exhibited nanoscale ZrO_2 dispersion, as seen in the magnified images [28, 29].

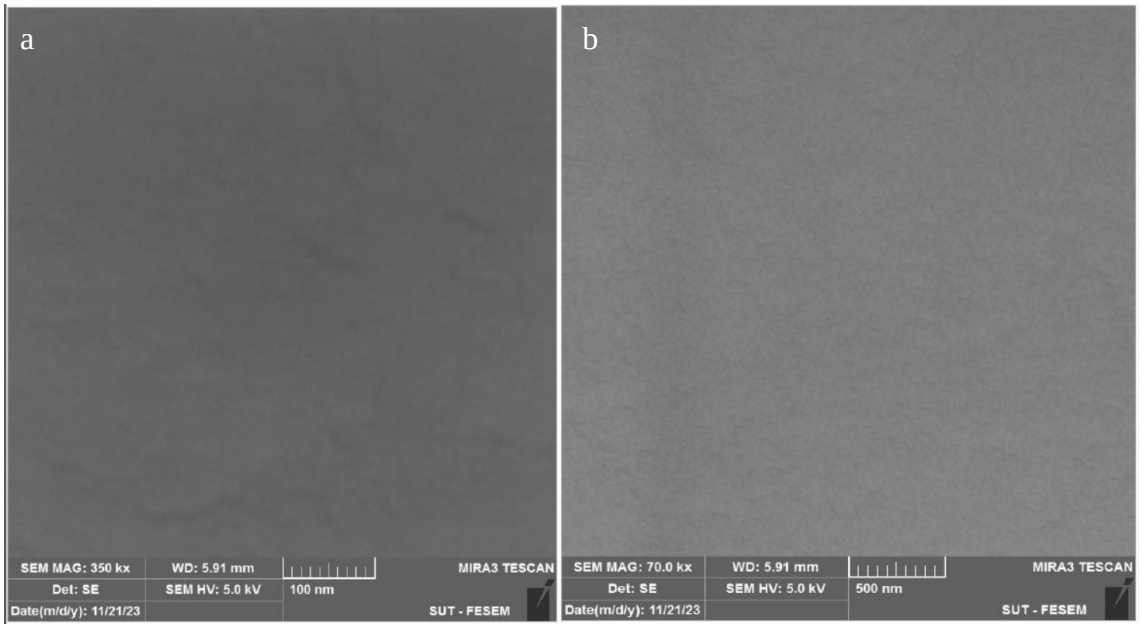

Figure 2: SEM images of the pure PLA/PCL film for (a) 100 nm, and (b) 500nm.

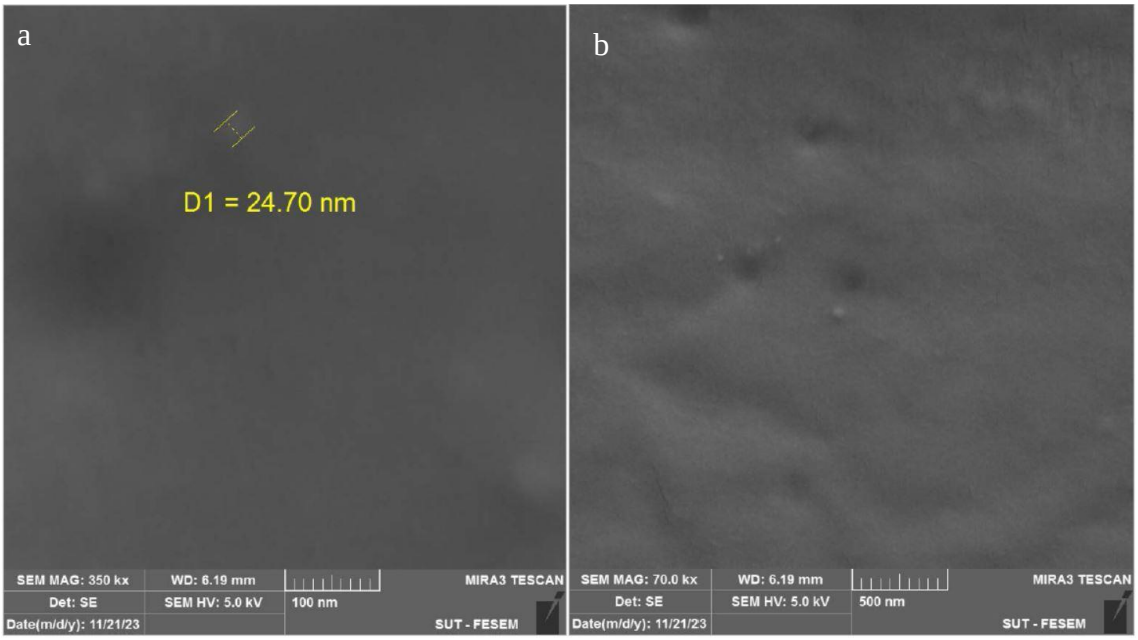

Figure 3: SEM images of PLA/PCL/0.75wt%ZrO_2NPs film for (a) 100 nm, and (b) 500nm..

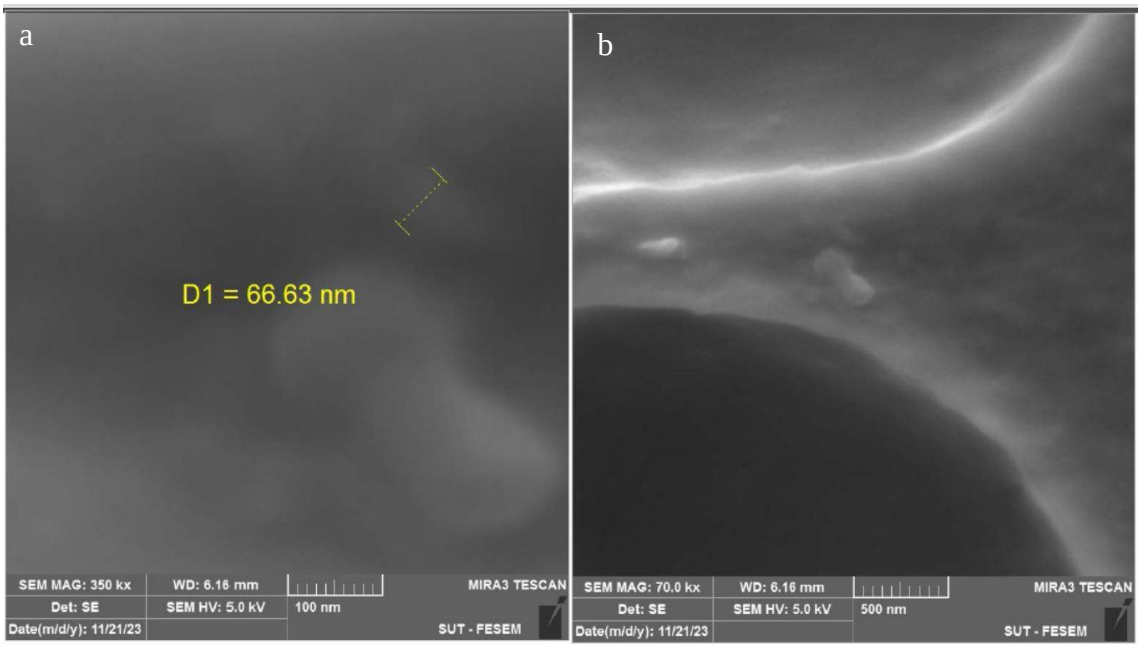

Figure 4: SEM images of PLA/PCL/1.5wt%ZrO_2NPs film for (a) 100 nm, and (b) 500nm.

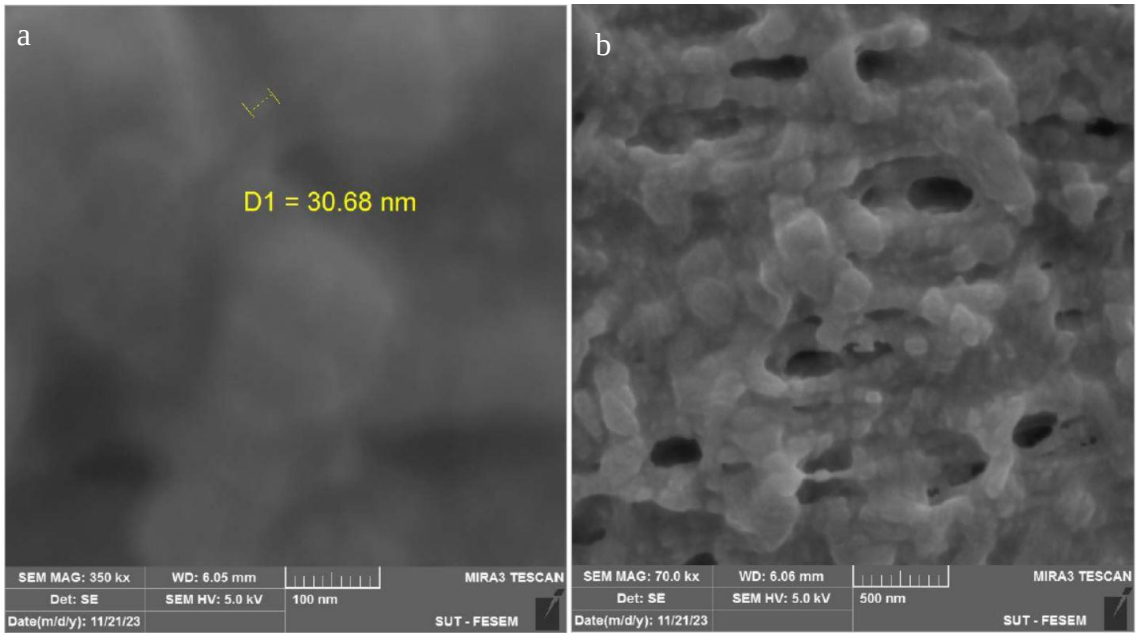

Figure 5: SEM images of PLA/PCL/2.25wt%ZrO_2NPs film for (a) 100 nm, and (b) 500nm.

3.3. DSC

The thermal behaviour of the pure PLA/PCL and PLA/PCL/ZrO_2NPs films was studied by the DSC. The DSC thermograms results are shown in Figs.6, 7, 8 and 9 and Table 2. The DSC study revealed that the glass transition and melting temperatures of the pure PLA/PCL were 93.03 °C and 100.59 °C, respectively. The glass transition temperature of PLA/PCL/ZrO_2NPs at ZrO_2NPs concentrations of 0.75 and 1.5wt% was decreased to 52.80 °C and 91.29 °C, respectively; the melting temperature was reduced to 61.19 °C and 99.07 °C, respectively. By incorporating ZrO_2NPs at a concentration of 2.25wt% into the PLA/PCL blend, the glass transition temperature increased to 101.87 °C, and the melting temperature increased to 130.03 °C. These findings suggest an enhanced degree of crystallinity, as confirmed by the XRD examination results when adding 2.25wt% ZrO_2NPs to the PLA/PCL blend [30, 31].

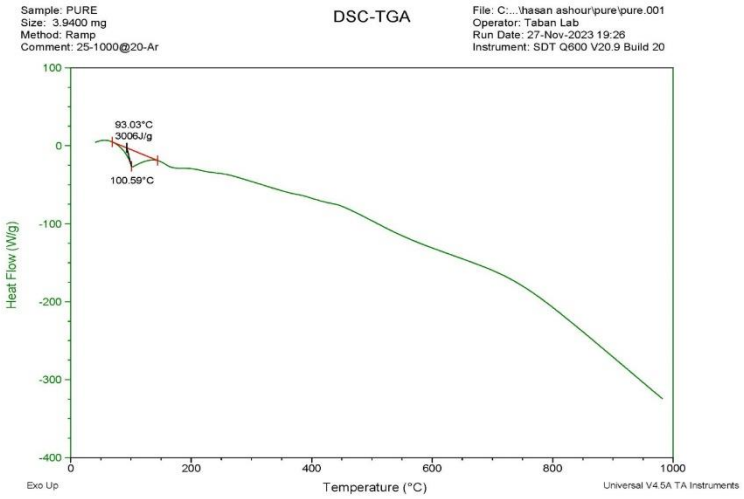

Figure 6: DSC thermogram of the pure PLA/PCL film.

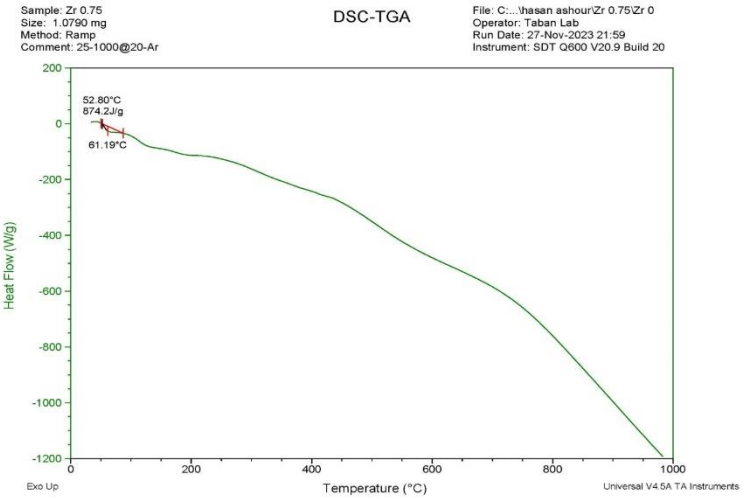

Figure 7: DSC thermogram of PLA/PCL/0.75wt%ZrO_2NPs film.

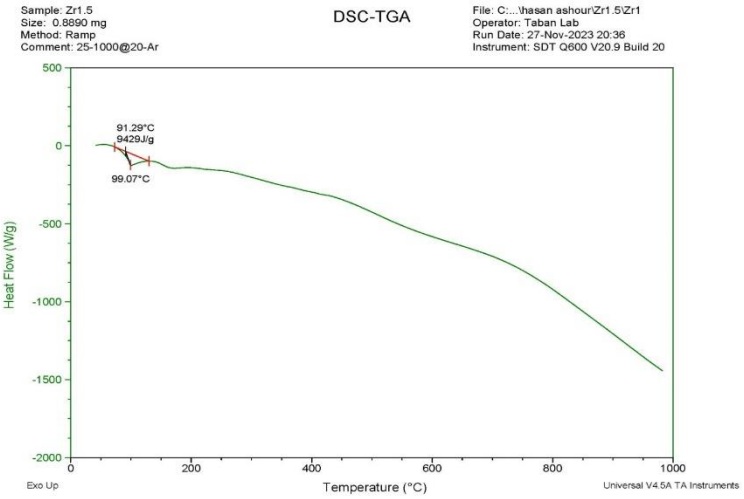

Figure 8: DSC thermogram of PLA/PCL/1.5wt%ZrO_2NP) film.

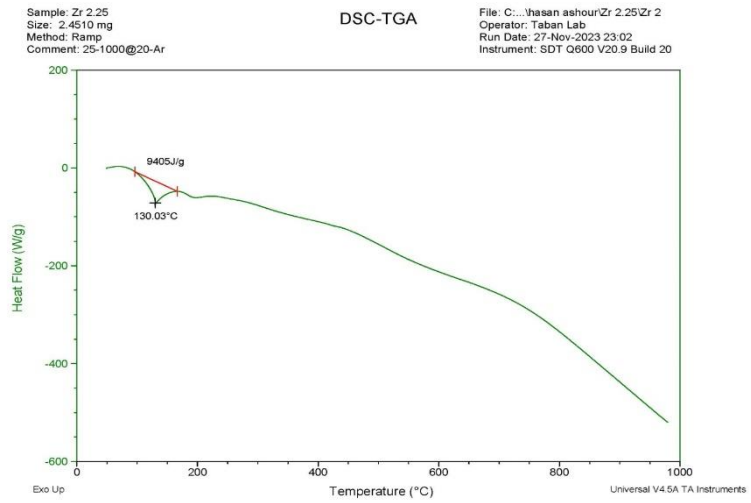

Figure 9: DSC thermogram of PLA/PCL/2.25wt%ZrO_2NPs.

Table 2: The glass transition and melting temperatures of the pure PLA/PCL, and PLA/PCL/ZrO_2NPs films.

Sample	**T_g**	**T_m**
Pure PLA/PCL	93.03	100.59
PLA/PCL/0.75wt%ZrO_2NPs	52.80	61.19
PLA/PCL/1.5wt%ZrO_2NPs	91.29	99.07
PLA/PCL/2.25wt%ZrO_2NPs	101.87	130.03

3.4. Antibacterial Activity

Staphylococcus aureus and Escherichia coli are the primary culprits behind foodborne illnesses. Fig. 10 demonstrates that PLA/PCL/2.25wt%ZrO_2NPs blend has a more pronounced antibacterial effect against Staphylococcus aureus bacteria than Escherichia coli bacteria. This could be explained by the broad range of morphological changes observed in bacterial cells. E. coli bacteria are more vulnerable to ZrO_2 nanoparticles because of their permeable and charged peptidoglycan surface [30].

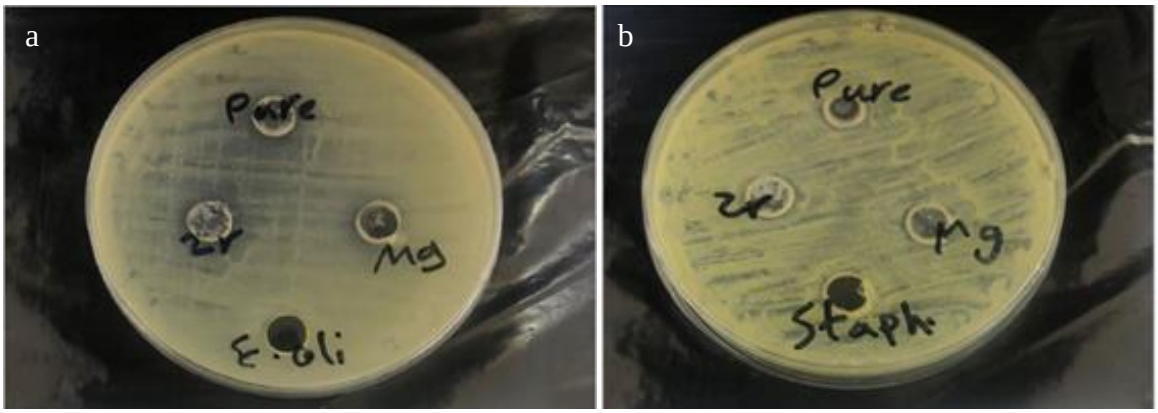

Figure 10: (a) Escherichia coli, (b) Staphylococeus aureus Antibacterial activity for the PLA/PCL/2.25wt%ZrO_2NP) blend.

4. Conclusions

This work presented PCL/PLA films reinforced with ZrO_2 NPs through a solvent-casting process. It is possible to conclude through the morphological and thermal tests that the reinforcement ratio greatly affects the properties of the blends. The results showed that random increases with an increase in the reinforcement ratio, which leads to a rise in the glass transition temperature and the melting point. Bacteriological efficacy tests show that ZrO_2 NPs has antibacterial properties. This is represented by its ability to interact with some biological and chemical factors in the surrounding environment, which inhibits the growth of germs and bacteria, making these films suitable for food packaging.

Conflict of interest

Authors declare that they have no conflict of interest.

References

1. I. Fortelny, A. Ujcic, L. Fambri, and M. Slouf, Sec. Poly. Comp. Mat. **6**, 1 (2019). DOI: 10.3389/fmats.2019.00206.
2. W. Lin, H. Shen, G. Xu, L. Zhang, J. Fu, and X. Deng, Comp. Part A Appl. Sci. Manufact. **115**, 22 (2018). DOI: 10.1016/j.compositesa.2018.09.008.
3. J. De Carvalho Arjona, M. Das Graças Silva-Valenzuela, S.-H. Wang, and F. R. Valenzuela-Diaz, Polymers **13**, 722 (2021). DOI: 10.3390/polym13050722.
4. C. G. Chiaregato, C. F. Souza, and R. Faez, Envir. Tech. Innovat. **22**, 101417 (2021). DOI: 10.1016/j.eti.2021.101417.
5. S. Sahani and Y. C. Sharma, Food Chem. **342**, 128318 (2021). DOI: 10.1016/j.foodchem.2020.128318.
6. J. Jeevanandam, A. Barhoum, Y. S. Chan, A. Dufresne, and M. K. Danquah, Beilstein J. Nanotech. **9**, 1050 (2018). DOI: 10.3762/bjnano.9.98.
7. I. M. Ali, A. A. Mohammed, and A. H. Ajil, Iraqi J. Phys. **14**, 191 (2016). DOI: 10.30723/ijp.v14i29.235.
8. A. Z. Naser, I. Deiab, and B. M. Darras, RSC Advances **11**, 17151 (2021). DOI: 10.1039/D1RA02390J.
9. B. U. Nam and Y. Son, J. Appl. Poly. Sci. **137**, 49011 (2020). DOI: 10.1002/app.49011.
10. D. Rasselet, M. F. Pucci, A.-S. Caro-Bretelle, J.-M. Lopez-Cuesta, and A. Taguet, Nanomaterials **11**, 1721 (2021). DOI: 10.3390/nano11071721.
11. T. Standau, C. Zhao, S. Murillo Castellón, C. Bonten, and V. Altstädt, Polymers **11**, 306 (2019). DOI: 10.3390/polym11020306.
12. X. Zhao, H. Hu, X. Wang, X. Yu, W. Zhou, and S. Peng, RSC Advan. **10**, 13316 (2020). DOI: 10.1039/D0RA01801E.
13. M. Delgado-Aguilar, R. Puig, I. Sazdovski, and P. Fullana-I-Palmer, Materials **13**, 2655 (2020). DOI: 10.3390/ma13112655.
14. A. H. Mohsen and N. A. Ali, Iraqi J. Sci. **63**, 4761 (2022). DOI: 10.24996/ijs.2022.63.11.15.
15. M. Catauro, E. Tranquillo, G. D. Poggetto, S. Naviglio, and F. Barrino, Macromolecular Symposia (Poland Wiley Online Library, 2020). p. 1900056.
16. C. Güneş Çimen, M. A. Dündar, M. Demirel Kars, and A. Avcı, ACS Biomat. Sci. Eng. **8**, 3717 (2022). DOI: 10.1021/acsbiomaterials.2c00611.
17. S. Beikzadeh, S. M. Hosseini, V. Mofid, S. Ramezani, M. Ghorbani, A. Ehsani, and A. M. Mortazavian, Int. J. Bio. Macromol. **191**, 457 (2021). DOI: 10.1016/j.ijbiomac.2021.09.065.
18. F. Maghfoori, N. Najmoddin, and M. Pezeshki-Modaress, Sci. J. Appl. Poly. **139**, e52684 (2022). DOI: 10.1002/app.52684.
19. P. J. Rivero, J. P. Fuertes, A. Vicente, Á. Mata, J. F. Palacio, M. Monteserín, and R. Rodríguez, Polymers **13**, 4312 (2021). DOI: 10.3390/polym13244312.
20. K. Hamad, M. Kaseem, M. Ayyoob, J. Joo, and F. Deri, Prog. Poly. Sci. **85**, 83 (2018). DOI: 10.1016/j.progpolymsci.2018.07.001.
21. S. Hussein, A. Abd-Elnaiem, N. Ali, and A. Mebed, Current Nanosci. **16**, 994 (2020). DOI: 10.2174/1573413716666200310121947.
22. M. Dadras Chomachayi, A. Jalali-Arani, F. R. Beltrán, M. U. De La Orden, and J. Martínez Urreaga, J. Poly. Envir. **28**, 1252 (2020). DOI: 10.1007/s10924-020-01684-0.

23. B. Al-Shabander, A. Mohammed, and H. Jaffer, Iraqi J. Sci. **54**, 105 (2013). DOI: https://ijs.uobaghdad.edu.iq/index.php/eijs/article/view/12038.
24. O. Okolie, A. Kumar, C. Edwards, L. A. Lawton, A. Oke, S. Mcdonald, V. K. Thakur, and J. Njuguna, J. Compos. Sci. **7**, 213 (2023). DOI: 10.3390/jcs7060213.
25. J. I. Castro, D. G. Araujo-Rodríguez, C. H. Valencia-Llano, D. López Tenorio, M. Saavedra, P. A. Zapata, and C. D. Grande-Tovar, Pharmaceutics **15**, 2196 (2023). DOI: 10.3390/pharmaceutics15092196.
26. C. Swaroop and M. Shukla, Mat. Today Proce. **5**, 20711 (2018). DOI: 10.1016/j.matpr.2018.06.455.
27. C. V. Reddy, B. Babu, I. N. Reddy, and J. Shim, Ceram. Int. **44**, 6940 (2018). DOI: 10.1016/j.ceramint.2018.01.123.
28. S. Solechan, A. Suprihanto, S. A. Widyanto, J. Triyono, D. F. Fitriyana, J. P. Siregar, and T. Cionita, Polymers **15**, 559 (2023). DOI: 10.3390/polym15030559.
29. M. Dadras Chomachayi, A. Jalali-Arani, and J. Martínez Urreaga, J. Poly. Envir. **29**, 2585 (2021). DOI: 10.1007/s10924-021-02053-1.
30. A. N. Obaid and N. Ali, Iraqi J. Phys. **18**, 1 (2020). DOI: 10.30723/ijp.v18i47.617.
31. A. N. Ali, M. A. Abd-Elnaiem, I. S. Hussein, S. A. Khalil, R. H. Alamri, and S. H. Assaedi, Curr. Nanosci. **17**, 494 (2021). DOI: 10.2174/1573413716999200820145518.

دراسة بعض الخصائص الفيزيائية والمضادة للبكتيريا للخليط الحيوي (PCL) / (PLA) مع جسيمات ZrO_2 النانوية

حسن علي عاشور[1] وعواطف عذاب محمد[1]

[1] قسم الفيزياء، كلية العلوم، جامعة بغداد، بغداد، العراق

الخلاصة

الهدف من هذه الدراسة إنتاج أغشية رقيقة من خلال مزج بين حامض البوليلاكتيك (PLA) والبولي كابرولاكتون(PCL)، وتعزيز قوتها من خلال تدعيمها بأوزان مختلفة (0.75, 1.5, 2.25 %) من الجسيمات النانوية (ZrO_2) باستخدام عملية الصب بالمذيبات. تم تحليل الخصائص الفيزيائية والمضادة للبكتيريا للأغشية لتحديد مدى ملاءمتها للاستخدام في تغليف المواد الغذائية. تحتوي أنماط حيود الأشعة السينية (XRD) لأغشية PLA / PCL ذات النسبة الوزنية 2.25٪ من جزيئات أكسيد الزركونيوم النانوية ذروة بزاوية $2\theta =$ 17.18°, مصحوبة بقمم أصغر. وهذا يؤكد أن هذه الاغشية الرقيقة تمتلك تركيبا شبه بلوري وان الجزيئات الموجودة في الأغشية الرقيقة منتشرة بشكل جيد. يكشف تحليل المجهر الإلكتروني الماسح (SEM) لأسطح الاغشية أن اغشية PLA/PCL النقية الغير مدعمة تظهر سطح أملس، في حين أن الاغشية الرقيقة المدعمة PLA/PCL/ZrO_2NPs لها سطح خشن بسبب التدعيم. قياس السعرات الحرارية بالمسح التفاضلي (DSC) أظهر السلوك الحراري للمادة تقلبات بسبب الاختلافات في نسبة التدعيم، مما أدى إلى تغيرات في كل من درجة حرارة انتقال الزجاج ونقطة الانصهار. تشير هذه التذبذبات إلى تغيرات في مستوى التبلور. يمتلك أكسيد الزركانيوم خصائص مضادة للجراثيم ومضادة للبكتيريا، مما يؤدي إلى تثبيط النمو، وهذا ما يجعل هذه الأغشية أكثر فعالية في تغليف المواد الغذائية.

الكلمات المفتاحية: حامض البولي لاكتيك، بولي كابرولاكتون، مضاد للبكتيريا، تغليف المواد الغذائية، مزيج حيوي.